End milling finite element method for cutting force prediction and material removal analysis

IOP Conf. Series: Materials Science and Engineering **788** (2020) 012020 doi:10.1088/1757-899X/788/1/012020

End milling finite element method for cutting force prediction and material removal analysis

Suraidah S[1], Muhamad Ridzuwan[1,*], Mebrahitom Asmelash[1], Azmir Azhar[1] and Freselam Mulubrhan[2]

[1] Faculty of Mechanical and Manufacturing Engineering, Universiti Malaysia Pahang
[2] Faculty of Industrial Management, Universiti Malaysia Pahang, Malaysia

[*]Corresponding e-mail: ridzuwan330@gmail.com

Abstract. The paper presents an orthogonal cutting finite element model analysis on Aluminum 6061 in order to investigate the effect of different number of cutting tool flutes (two and four) on the von misses stress distribution and analysis of cutting forces in three force direction which are in $\mathbf{F_x}$, $\mathbf{F_y}$, $\mathbf{F_z}$. The machining parameters used in the simulation and experiment was a depth of cut of 3 mm and 6 mm with a recommended machining parameter, a 2-flute and 4- flute end mill cutter used for each case. The results showed that the simulation and experiment indicated that the predicted and the measured cutting force of milling process are in a good agreement and the shape of the chip generated was similar.

Keywords. End milling; orthogonal cutting; finite element analysis

1. Introduction

Aluminium alloy 6061 is one of the versatile material which is commonly used in the transportations, part component in machineries and medical equipment and because of its range of mechanical strength and toughness properties and very good corrosion resistance in its industrial applications [1-3]. Although it has a considerable very good machinability compared to other similar materials, it is reported that machine shops have a number of specifictabl concerns when it comes to working with this material, including long, stringy chips, chips wrapping on parts, machined surface finish, rough thread finish, dimensions [4]. This calls for the machining predictions and appropriate use of machining parameters. End milling is one of the common methods in machining of aluminium 6061 because of its capability and versatility to produce various profiles, curve, and surfaces. The quality of end milling machining is affected by the geometry and of cutting flutes and the surface of the end mill.

For the appropriate selection of machining parameters such spindle speed, feed rate, depth of cut, the prediction of cutting forces is very important [5] and helps the machine tool industry in cost reduction and productivity. End mill design requires the perfect analysis of tool surface geometry and cutting forces along with cutting flutes [6, 7].

In a linear milling process the tool path is assumed to be straight so that the feed rate at each cutting points along the cutter circular path keeps constant and equal to the normal feed rate f. which refers to the feed per tooth.

The first step is to divide the cutting flute in to a number of differential elements along the flute profile so that so that each of the forces acting on the elements is numerically integrated to calculate the total force on the flute. As shown in Equation 1, three orthogonal force components [6] in Cartesian coordinates system of i^{th} cutter element for j^{th} tooth can be obtained by following transformation of the tangential, radial and axial forces defined on the cutting flute element [8].

$$\begin{pmatrix} dF_{i,j,X(\emptyset_{i,j},z)} \\ dF_{i,j,Y(\emptyset_{i,j},z)} \\ dF_{i,j,Z(\emptyset_{i,j},z)} \end{pmatrix} = \mathrm{M} \begin{pmatrix} dF_{i,j,T} \\ dF_{i,j,R} \\ dF_{i,j,A} \end{pmatrix} \tag{1}$$

Where,

$$\mathrm{M} = \begin{matrix} -\cos\emptyset_{i,j} & -\sin\emptyset_{i,j} & 0 \\ sin\,\emptyset_{i,j} & cos\,\emptyset_{i,j} & 0 \\ 0 & 0 & -1 \end{matrix}$$

The total force acting on the j^{th} cutting edge can be obtained by integrating along the axial depth of cut:

$$F_j = \int_{z_1}^{z_2} dF_j \; d_z$$

And z_1, z_2 depend on the immersion condition of j^{th} tooth. Finally the total cutting forces on the milling cutter in feed (X), normal (Y) and axial (Z) directions are obtained by summing the contribution of all cutting edges.

$$f_{x,y,z} = \sum_{j=1}^{N_f} F_j$$

Kahled et al. [9] developed and compared the analytical models of linear and non-linear forces. It was demonstrated that the nonlinear force models were seen good approximation compared linear models determined using the force coefficients by Altintas and Budak [10, 11]. On the other hand, Baohai et al. [12] developed circular end milling cutting model based on the traditional linear cutting model. Experimental results showed that measured results and simulated results corresponds well with each other. The consideration of curvature effects of tool path on chip thickness as well as entry and exit angles contributed to the better accuracy the forces compared to the linear models. However, the computational complexity and time make it difficult in using nonlinear models as linear model requires less time and optimum operational requirements. The computational time to finish the simulation operation can raise the cost and time consumption in the industry. In this paper a finite element analysis simulation model was developed and cutting forces acting on the end mill was predicted.

2. Numerical formulation

For the linear end milling process, a commercial software code, ABAQUS/Explicit v6.4 and ALE modelling approach is used to conduct the FEM simulation of orthogonal cutting considering. In the numerical study performed, the Johnson–Cook material model [13] was used as the work piece material model. The material is aluminium 6061 alloy and the cutting tool was high speed steel with two and four flute geometry. The material properties are listed in table 1. The Johnson–Cook material model was employed in this study, which is represented by equation (2) [14]:

$$\bar{\sigma} = [A + B(\bar{\varepsilon})^n]\left[1 + C\ln\left(\frac{\bar{\varepsilon}}{\dot{\bar{\varepsilon}}_0}\right)\right]\left[1 - \left(\frac{T - T_{room}}{T_{melt} - T_{room}}\right)^m\right] \quad (2)$$

where $\bar{\sigma}$ is the equivalent flow stress, ε is the equivalent plastic strain, ε and ε· is the equivalent plastic strain rate, $\bar{\varepsilon}/\varepsilon_o$ is the reference equivalent plastic strain rate, T is the work piece temperature, T_{melt} is the material melting temperature, and T_{room} is the room temperature. This model is widely used for the analysis of material flow stress, especially for those materials where flow stress is highly influenced by temperature and strain rate. Johnson–Cook parameters developed by Lesuer [15] are used in this study, as listed in table 2 and 3.

Table 1. Mechanical and physical properties for Aluminium 6061[16].

	Tool	Work piece
Modulus of Elasticity, E(GPa)	200 GPa	70
Poisson's ratio, v	0.33	0.3
Density, ρ (Kg/cm^3)	7870	2700 kg/m^3
Specific Heat capacity, Cp (J/Kg. ^{o}c)	.477	.885
Thermal conductivity, K (W/m ^{o}c)	44.5	167
Melting temperature, T (^{o}c)	1520	582-652
Linear thermal coefficient of expansion, ξ (µm/m ^{o}c)	12.3	25.2
Displacement at Failure	0.1	0.0001

Table 2. Johinson Cook plasticity material constants of aluminium 6010 and the tool [2].

	A (MPa)	B(MPa)	n	C	m
Aluminium 6061	3.241e8	1.138e8	.42	.002	1.34
HSS tool	375e6	552e6	.457	.014	1.03

Table 3. Johinson Cook Damage material constants of Aluminium 6010 and the tool.

	D1	D2	D3	D4	Reference Strain Rate
Aluminium 6061	-0.77	1.45	-0.47	0	1
HSS tool	.25	4.38	2.68	0	1

3. Experimental set up

An end milling machining was performed for the validation which is a Vertical milling machine model Makino (M11-KE55P00/2) being conducted to obtain the real results of the experiments. The experiments are conducted three times in order to get the average value, thus increasing the accuracy of the value obtained.

A high-speed steel end mill tool cutter of 10 millimeters with two and four flutes was used to with an aluminum work piece of dimension of 100 millimeters x 100 millimeters x 20 millimeters. The strain-based gauge dynamometer was used to evaluate the cutting forced produced during the experiment. A force dynamometer connected to the amplifier was used for the force data collection using the acquisition system as shown in figure 1a and b.

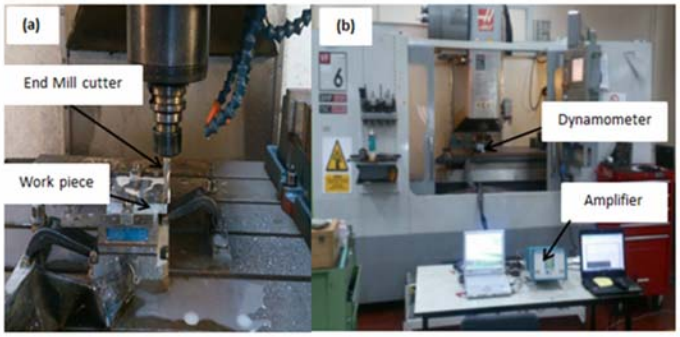

Figure 1. Experimental set up during the force data acquisition.

Simulation modelling has been executed with the machining parameters stated in the table 4 where the input parameters used in both the experiment and simulation, a total of six scenarios.

Table 4. Parameter of the experimental investigation.

Tests	Spindle speed, Rpm	Depth of cut d, mm	Feed Rate F, mm/min	*2 Flutes	*4 Flutes
1	1300	3	46	Fx, Fy, Fz	Fx, Fy, Fz
2	1300	6	85	Fx, Fy, Fz	Fx, Fy, Fz

*Fx = Radial force, *Fy = Tangential force, *Fz =Axial force.

4. Results and discussion

The simulated results were compared with the forces measured using the force dynamometer. In each case of the scenario, using a two flute and four flute cutters, the three component forces were compared. As shown in table 4, the parameters used in the first types of experiment are spindle speed of 1300 rpm, 3 mm depth of cut, 46 mm/min feed rate and 1300 rpm, 6 mm depth of cut, 85 mm/min feed rate fo
r two and four flute cutters respectively. Figures 2a and 2b show the comparison of simulation and experimental end milling cutting forces for two flute and 4 flute cutter of the radial forces when the depth of cut is 3mm. Similarly, Figures 3a and 3b show the comparison of simulation and experimental end milling cutting forces for two flute and 4 flute cutter of the radial forces when the depth of cut is 6 mm. Figures 4 and 5 also show the cutting forces with 3 and 6 mm depth of cut when used the two flute and 4 flute end mill. In both cases, it is observed that as the depth of cut increases the cutting forces showed higher which is true from the practical point of view. It can be also observed that the four flute cutter generated less force value in either direction of the tool than the two flute. In fact, the tool will be tougher or increase in its rigidity if the number of flute increases as well feed faster.

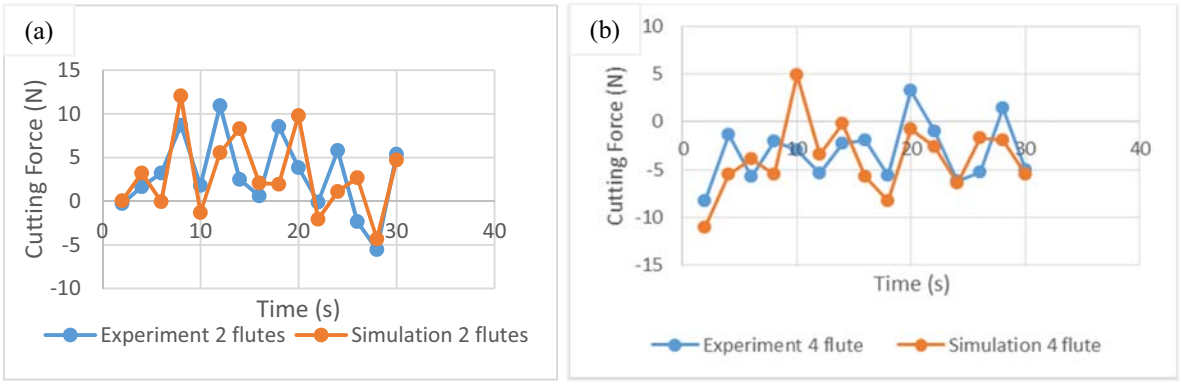

Figure 2. Comparison of radial force (Fx) of experimental & simulation results compared of (a) 2 flute (b) 4 flutes end milling for 3 mm depth of cut.

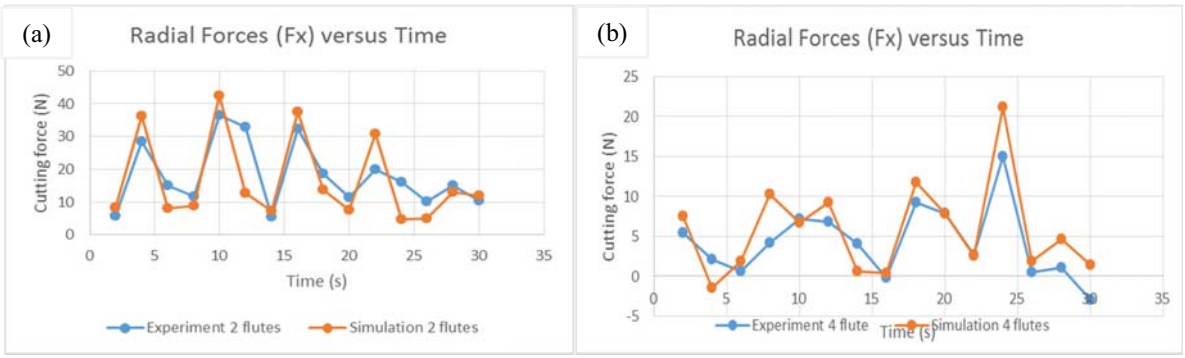

Figure 3. Comparison of Tangential force (Fx) of experimental & simulation results compared of (a) 2 flute (b) 4 flutes end milling for 6 mm depth of cut.

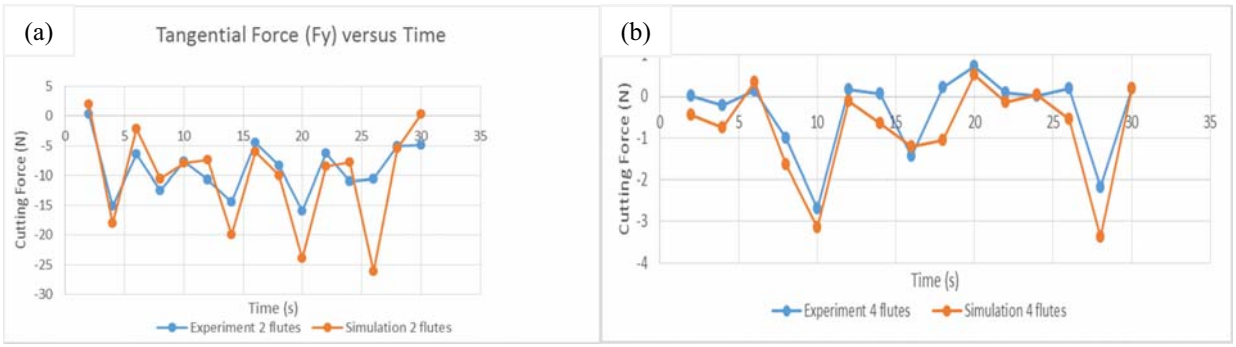

Figure 4. Comparison of Tangential force (Fx) of experimental & simulation results compared of (a) 2 flute (b) 4 flutes end milling for 3 mm depth of cut.

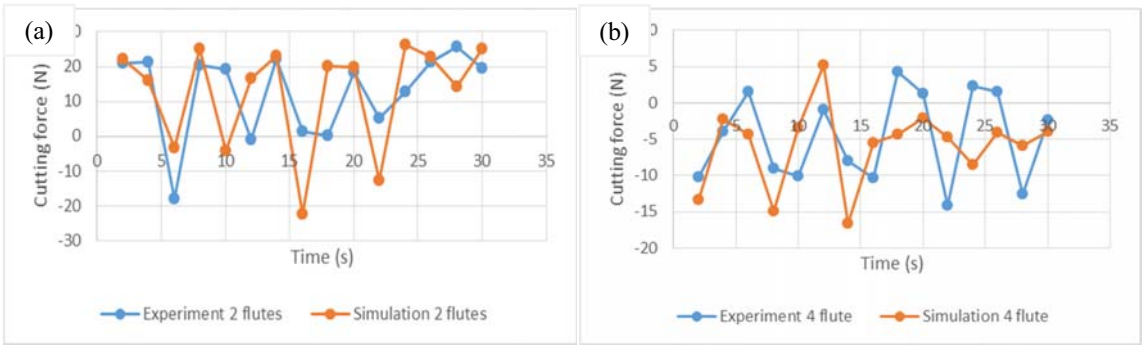

Figure 5. Comparison of Tangential force (Fx) of experimental & simulation results compared of (a) 2 flute (b) 4 flutes end milling for 6 mm depth of cut.

The cutting force analysis shows that the predicted and experimentally measured forces are in good agreement with an error in the range of 20- 30 % in all force directions. Figure 6 shows the chips shape and surface texture at a feed rate of 46 mm/min, axial depth of cut 3 mm and with cutting speed of 47 m/min which may be taken of similarity between the simulation and actual machining during the chip formation which is a continuous shape formed. In summary, the prediction of cutting forces using finite element analysis brings better benefit that it reduces the cost of tool failure in the industry.

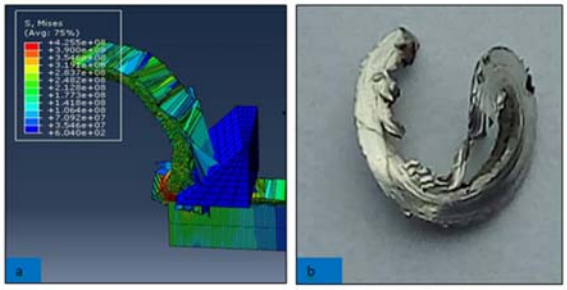

Figure 6. Chip formation formed in simulation (a) and experiment from the third trial (b). The simulation and experiment shows the continuous chip formed.

5. Conclusion

Using a finite element analysis simulation model of different scenarios, cutting force was studied and compared with the experimental results. The simulated data showed that increasing the depth of cut from 3 mm to 6 mm increases the force generated. The use of higher number flutes showed that the force generated per flute decreases. It was also observed that the shape of the simulated chip shape was approximately of the same curvature and shape with the experimental results.

Acknowledgement

This research was supported by research grant RDU1703193 from University Malaysia Pahang.

References

[1] Mebrahitom, A., W. Choon, and A. Azhari, *Side Milling Machining Simulation Using Finite Element Analysis: Prediction of Cutting Forces.* Materials Today: Proceedings, 2017. **4**(4, Part D): p. 5215-5221.

[2] Piekutowski, A.J., et al., *Perforation of aluminum plates with ogive-nose steel rods at normal and oblique impacts.* International Journal of Impact Engineering, 1996. **18**(7): p. 877-887.

[3] Hao, M., D. Xu, and P. Feng, *Numerical and experimental investigation of the shear angle in high-speed cutting of Al6061-T6.* The International Journal of Advanced Manufacturing Technology, 2019. **100**(9): p. 3037-3044.

[4] Kuttolamadom, M., S. Hamzehlouia, and L. Mears, *Effect of Machining Feed on Surface Roughness in Cutting 6061 Aluminum.* SAE International Journal of Materials and Manufacturing, 2010. **3**(1): p. 108-119.

[5] Gebremariam, M.A., et al., Remaining Tool Life Prediction Based on Force Sensors Signal During End Milling of Stavax ESR Steel. 2017(58356): p. V002T02A094.

[6] Mamalis, A., et al., *Finite element simulation of chip formation in orthogonal metal cutting.* Journal of Materials Processing Technology, 2001. **110**(1): p. 19-27.

[7] Mebrahitom, A., et al. Effect of High-speed Milling tool path strategies on the surface roughness of Stavax ESR mold insert machining. in IOP Conference Series: Materials Science and Engineering. 2016. IOP Publishing.

[8] Saptaji, K., M.A. Gebremariam, and M.A.B.M. Azhari, *Machining of biocompatible materials: a review.* The International Journal of Advanced Manufacturing Technology, 2018. **97**(5): p. 2255-2292.

[9] Adem, K.A., R. Fales, and A.S. El-Gizawy, Identification of cutting force coefficients for the linear

and nonlinear force models in end milling process using average forces and optimization technique methods. The International Journal of Advanced Manufacturing Technology, 2015. **79**(9-12): p. 1671-1687.

[10] Altintas, Y., Manufacturing automation: metal cutting mechanics, machine tool vibrations, and CNC design. 2012: Cambridge university press.

[11] Budak, E., Y. Altintas, and E. Armarego, *Prediction of milling force coefficients from orthogonal cutting data.* Journal of Manufacturing Science and Engineering, 1996. **118**(2): p. 216-224.

[12] Wu, B., et al., *Cutting force prediction for circular end milling process.* Chinese Journal of Aeronautics, 2013. **26**(4): p. 1057-1063.

[13] Bajpai, V., I. Lee, and H.W. Park, *Finite element modeling of three-dimensional milling process of Ti–6Al–4V.* Materials and Manufacturing Processes, 2014. **29**(5): p. 564-571.

[14] Asad, M., et al., Dry cutting study of an aluminium alloy (A2024-T351): a numerical and experimental approach. International Journal of Material Forming, 2008. **1**(1): p. 499-502.

[15] Lesuer, D.R., G. Kay, and M. LeBlanc, *Modeling large strain, high rate deformation in metals.* Engineering research, development and technology, 1999.

[16] Gupta, N.K., M.A. Iqbal, and G.S. Sekhon, Experimental and numerical studies on the behavior of thin aluminum plates subjected to impact by blunt-and hemispherical-nosed projectiles. International Journal of Impact Engineering, 2006. **32**(12): p. 1921-1944.